

Intelligent Control of a SPM System Design with Parameter Variations

Jium-Ming Lin and Po-Kuang Chang

Abstract—This research is to use fuzzy controller in the outer-loop to reduce the hysteresis effect as well as parameter variations of a force actuator for a Scanning Probe Microscope (SPM). This improvement has been verified by practical implementation. Comparisons with a previous design for the outer-loop with PI compensator and inner-loop with Linear Velocity Transducer (LVT) for feedback compensation are also made. Thus the proposed system is more robust.

Index Terms—Fuzzy controller, SPM, Hysteresis effect, LVT.

I. INTRODUCTION

The SPM has been developed rapidly in last three decade [1]–[10]. Its usage is very extensive, e. g. the measurements of physical distribution and material property such as surface profile, roughness, static charge, magnetic dipole, friction, elasticity, and thermal conductivity. As the block diagrams in Fig. 1 of previous research [11], a balance with stylus probe, force actuator, LVDT, load cell, personal computer, and XYZ-stages were integrated into a contact force-controlled SPM, such that the surface of the sample would not be destroyed by the stylus probe. To reduce the hysteresis effect of the force actuator as well as parameter variations this research in Fig. 2 applied a fuzzy controller [12]–[15] in the outer-loop and LVT in the feedback loop to reduce the force actuator hysteresis effect of a SPM.

This improvement has been verified by practical implementation of a surface profiler. Comparisons with the previous design for the outer-loop with PI compensator and with LVT for inner-loop feedback are also made. Thus the proposed system is more robust.

The organization of this paper is as follows: the first section is introduction. The second and the third ones are respectively for the review of previous research and the proposed fuzzy controller design. The test results and discussions are given in Section 4. The last part is the conclusion.

Manuscript received January 11, 2010. (Write the date on which you submitted your paper for review.) This work was supported in part by National Science Council of R. O. C. under Grant NSC 97-2221-E-216-013-MY2.

J. M. Lin is with the Department of Communication Engineering, Chung-Hua University, Hsin-Chu, 30012 TAIWAN (corresponding author phone: 886-3518-6483; fax: 886-3518-6521; e-mail: jmlin@chu.edu.tw).

P. K. Chang is a Ph. D. candidate of Ph.D. Program in Engineering Science, College of Engineering, and Chung-Hua University, Hsin-Chu, 30012 TAIWAN. (e-mail: puppy@itri.org.tw).

II. REVIEW OF PREVIOUS SYSTEM DESIGN

The force actuator is consisted of a coil and a spring, as in Fig. 3(a) the rod returns to the initial place when the force actuator de-energized, when a voltage is applied across the coil, then there is current in the coil, and a force is generated to compress the spring and make the rod pull down as in Fig. 3(b).

The relationship of the applied voltage and displacement is shown in Fig. 4. To reduce the hysteresis effect of the force actuator in Fig. 4, this research is to use a fuzzy controller to replace the PI compensator for a previous research, the newly system model is shown in Fig. 2. Table I listed the previous PI compensators [11] for inner and outer loops design (steady state errors are equal to zero for inner and outer loops) in Fig. 1. In addition, the gain margins, phase margins of the inner (GM1, PM1) and outer (GM2, PM2) loops as well as the phase crossover frequency ω_c are also included.

Figs. 5-8 are the Bode plots of cases 1, 2, 5 and 6, respectively. The outputs of LVDT for saw tooth shaped input (as in Fig. 9) are shown from Figs. 10 to 13 for comparison (with hysteresis effect parameter D be 0.3). One can see that the larger the outer-loop phase margin, the lower the hysteresis effect, but all the hysteresis effects are still very dominant. The reason is ω_c are very large for these cases, and then the time and phase delays produced by the hysteresis effect would be increased. Thus the stability can even be degraded by adding the hysteresis effect to push the resulting phase margins zero.

III. FUZZY CONTROLLER DESIGN

A. Relationship Functions Design

In this section a Proportion and Derivative (PD) type fuzzy controller [12] – [15] is applied in the forward loop as in Fig. 2. It is well-known that fuzzy controller is based on the IF-THEN RULE as follows:

R1: IF E is NB AND ΔE is NB THEN U is NB,
R2: IF E is NB AND ΔE is ZE THEN U is NM,
R3: IF E is NB AND ΔE is PB THEN U is ZE,
R4: IF E is ZE AND ΔE is NB THEN U is NM,
R5: IF E is ZE AND ΔE is ZE THEN U is ZE,
R6: IF E is ZE AND ΔE is PB THEN U is PM,
R7: IF E is PB AND ΔE is NB THEN U is ZE,
R8: IF E is PB AND ΔE is ZE THEN U is PM,
R9: IF E is PB AND ΔE is PB THEN U is PB,

where NB, NM, NS, ZE, PS, PM, and PB respectively stand for negative big, negative middle, negative small, zero, positive small, positive middle and positive big.

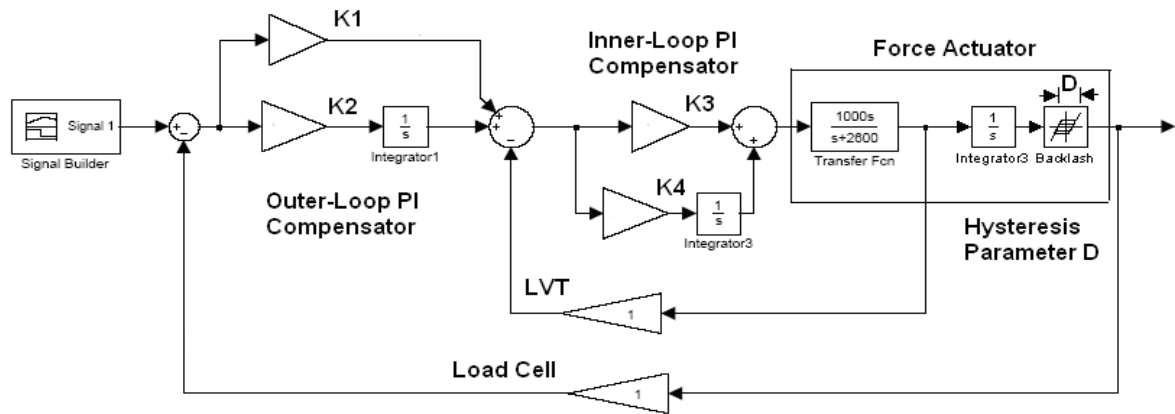


Fig. 1 Block diagram of SPM with LVT for inner-loop feedback in the previous research [11].

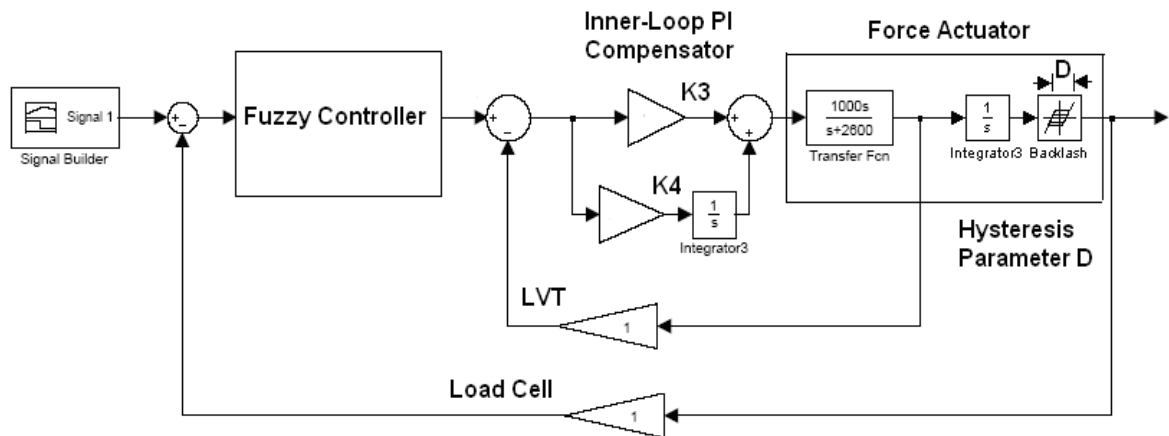


Fig. 2 Block diagram of SPM with a fuzzy controller in the outer-loop and LVT in the feedback loop of this research.

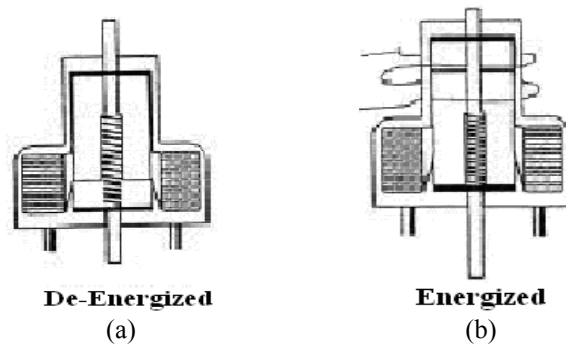


Fig. 3 Actuator operation states.

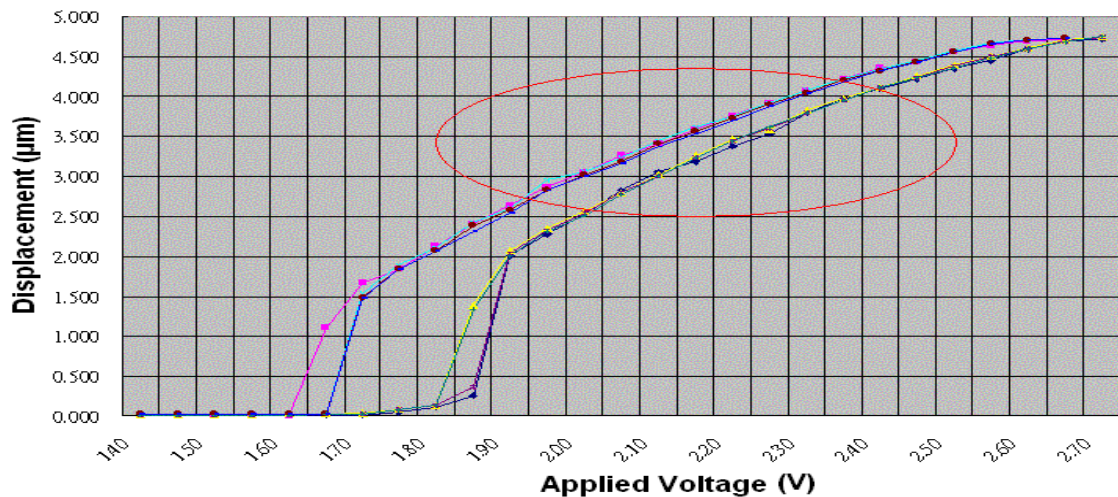


Fig. 4 Actuator applied voltage vs. displacement

Table I
 Previous design results of system in Fig. 1.

Case	K1	K2	K3	K4	GM1	PM1 (Deg)	GM2	PM2 (Deg)	ω_c (r/sec)
1	12	120	1	200	∞	73	∞	85	9840
2	10	100	0.8	180	∞	75	∞	70	7500
3	15	100	1.5	200	∞	65	∞	88	20000
4	20	150	2	150	∞	63	∞	89.5	40000
5	8	80	0.5	300	∞	85	∞	60	30000
6	18	200	1.3	220	∞	70	∞	90	30000

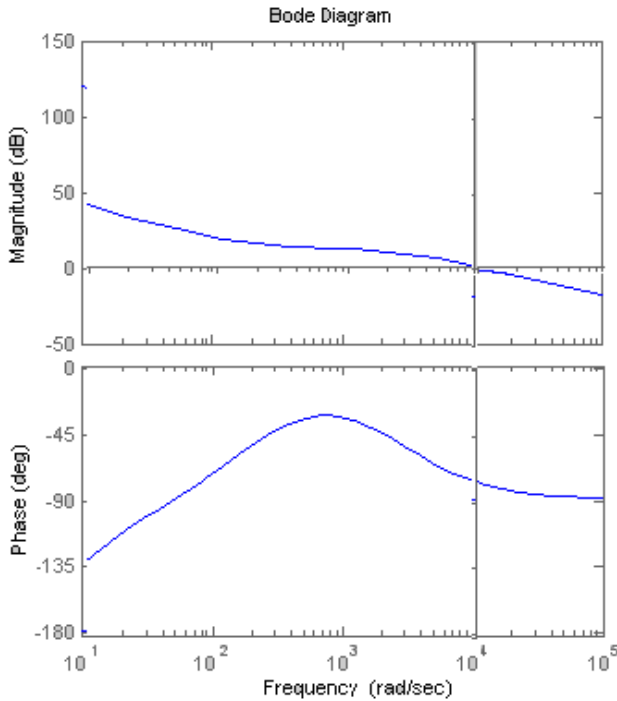


Fig. 5 Previous Bode plot of case 1 in Fig. 1.

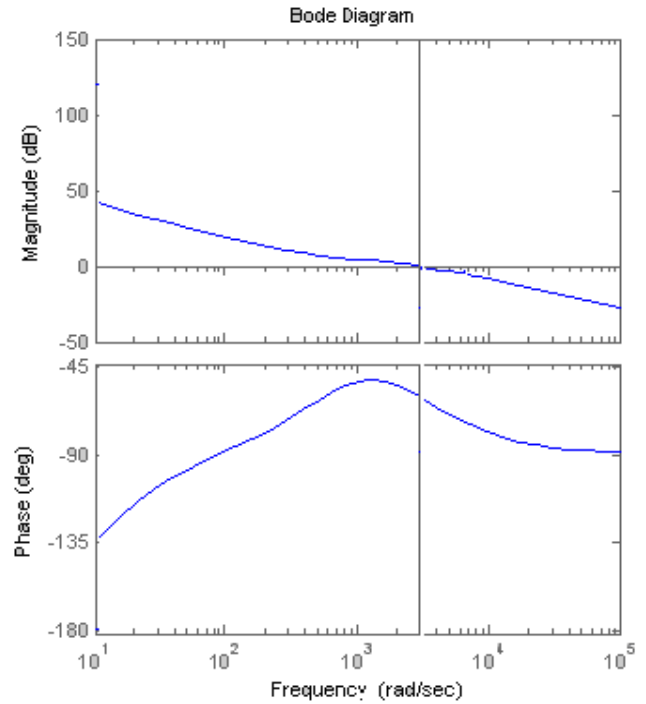


Fig. 7 Previous Bode plot of case 5 in Fig. 1.

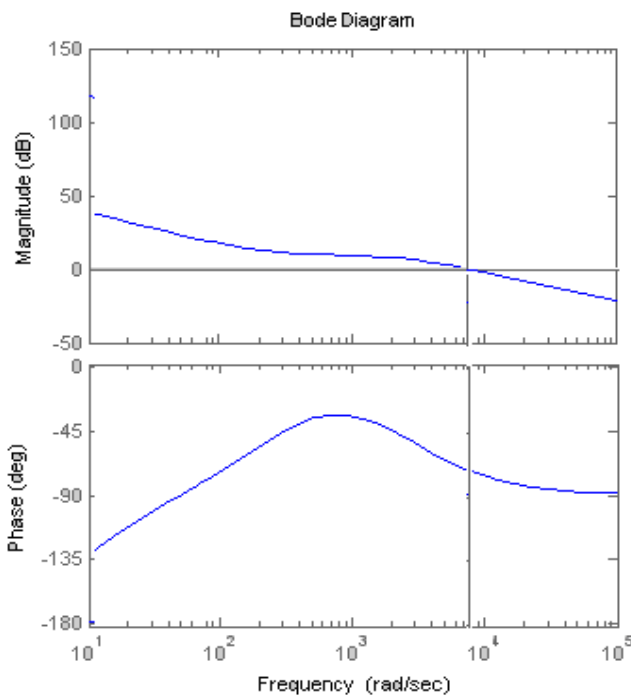


Fig. 6 Previous Bode plot of case 2 in Fig. 1.

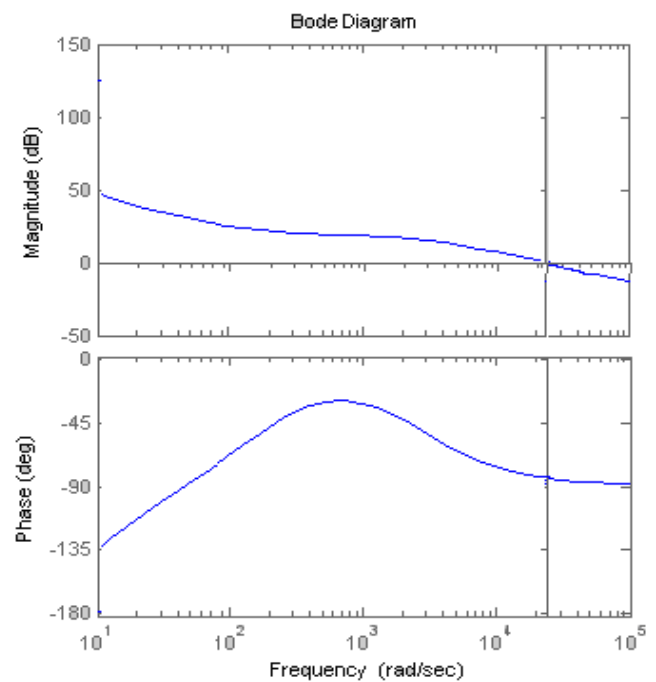


Fig. 8 Previous Bode plot of case 6 in Fig. 1.

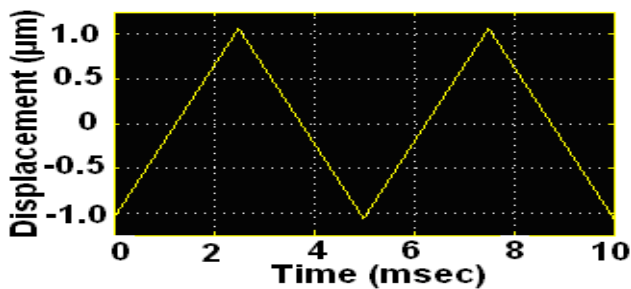


Fig. 9 A saw tooth shaped displacement command as input.

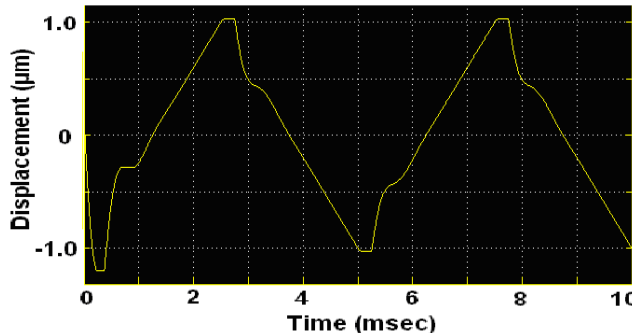


Fig. 12 Previous design output of case 5 in Fig. 1 (D = 0.3).

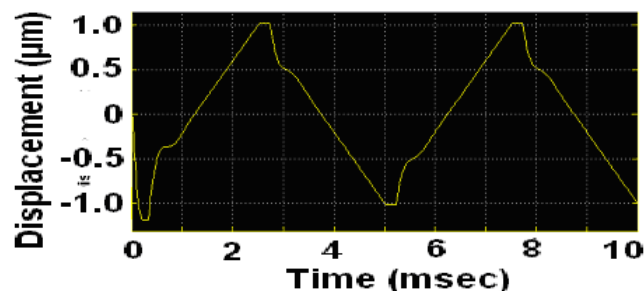


Fig. 10 Previous design output of case 1 in Fig. 1 (D = 0.3).

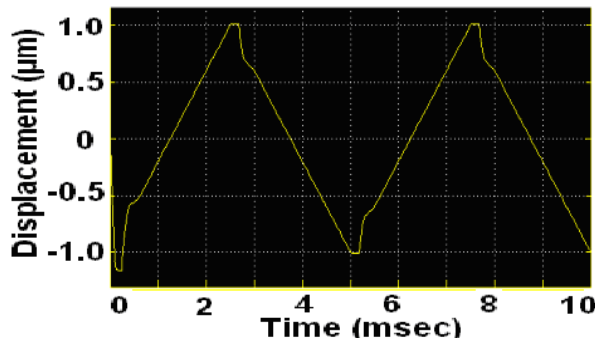


Fig. 13 Previous design output of case 6 in Fig. 1 (D = 0.3).

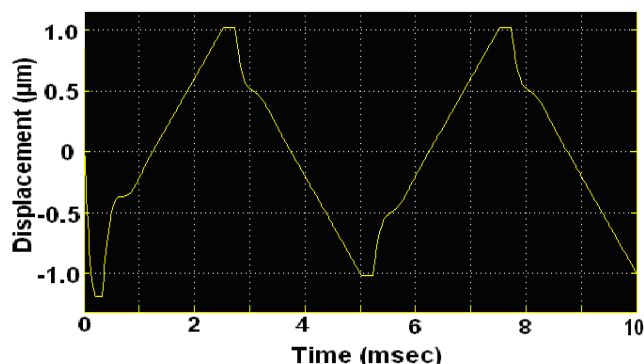


Fig. 11 Previous design output of case 2 in Fig. 1 (D = 0.3).

Table II. Fuzzy controller cross reference rules.

E/ΔE	NB	NM	NS	ZE	PS	PM	PB
NB	NB	NB	NM	NM	NS	NS	ZE
NM	NB	NM	NM	NS	NS	ZE	PS
NS	NM	NM	NS	NS	ZE	PS	PS
ZE	NM	NS	NS	ZE	PS	PS	PM
PS	NS	NS	ZE	PS	PS	PM	PM
PM	NS	ZE	PS	PS	PM	PM	PB
PB	ZE	PS	PS	PM	PM	PB	PB

The detailed cross reference rules for the inputs and output of fuzzy controller are defined in Table II. According to fuzzy control design method the membership function parameters of error E, ΔE (deviations of present E and the previous E), and U (control input) are defined at first, which are listed in

Table III. To reduce the computation time the triangular distribution functions are applied in fuzzy controller relationship functions calculation instead of using the traditional Gaussian ones.

Table III. Fuzzy controller cross reference rules.

Item	Parameter E	Parameter ΔE	Parameter U
Negative Big (NB)	[-1 -1 -0.75 -0.3]	[-4.5 -4.5 -3.375 -1.35]	[-12 -12 -9.6 -8.4]
Negative Medium (NM)	[-0.75 -0.3 -0.15]	[-3.375 -1.35 -0.72]	[-9.6 -8.4 -7.2]
Negative Small (NS)	[-0.15 -0.1 0]	[-1 -0.5 0]	[-8.4 -4.8 0]
Zero (ZE)	[-0.05 0 0.05]	[-0.25 0 0.25]	[-4.8 0 4.8]
Positive Small (PS)	[0 0.1 0.15]	[0 0.5 1]	[0 4.8 8.4]
Positive Medium (PM)	[0.15 0.3 0.75]	[0.72 1.35 3.375]	[7.2 8.4 9.6]
Positive Big (PB)	[0.3 0.75 1 1]	[1.35 3.375 4.5 4.5]	[8.4 9.6 12 12]

B. Fuzzy Controller Performance Analysis

Fig. 14 shows the response (D = 0.3). It can be seen that the hysteresis effect is almost disappeared, so that this method is better than those obtained by the previous PI controllers.

In addition, if there is a parameter variation in the actuator for larger backlash effect, e. g. D = 0.5, the result is still very good as in Fig. 15. However, the result of the previous design is as in Fig. 16, which is very bad.

On the other hand, since the force produced by the current of voice coil is:

$$F = B\ell i \tag{1}$$

The applied force F produced by the current is also equal to the spring constant k times the compression displacement x:

$$F = kx \tag{2}$$

The relationship of the phasor-voltage and phasor-current for the voice coil is:

$$V(s) = I(R + j\omega L) \tag{3}$$

where R and L are the resistance and inductance of voice coil, respectively. Thus one has the transfer function of the voice coil force actuator be obtained as:

$$\frac{X}{V} = \frac{B\ell k}{R + j\omega L} = \frac{B\ell k}{s + \frac{R}{L}} \quad (4)$$

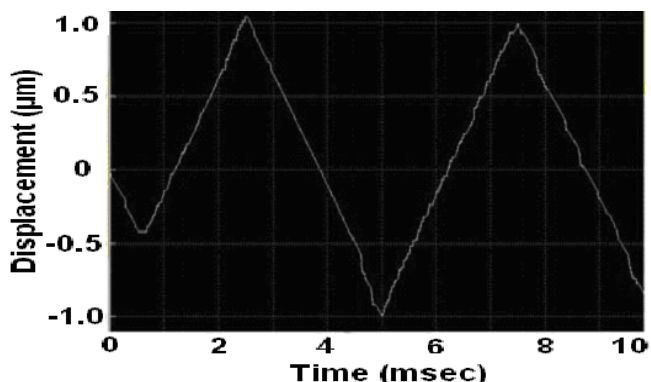


Fig. 14 The output response with fuzzy controller ($D = 0.3$).

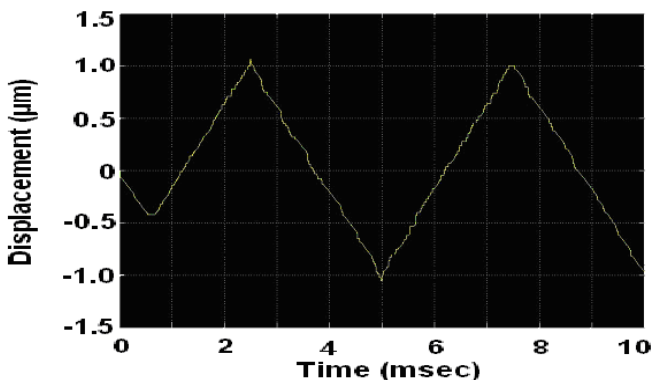


Fig. 15 The output response with fuzzy controller ($D = 0.5$).

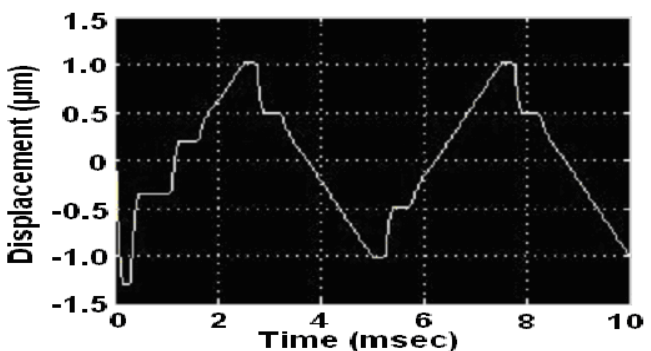


Fig. 16 The output response of the previous design ($D = 0.5$).

If the resistance of the voice coil is increased for long time operation and the temperate effect, then the value of R/L in the denominator would be increased, i. e. the nominal value of R/L is changed from 2600 to 3900. Then the output response with fuzzy controller is as in Fig. 17, one can see the result of the new method is still very good.

If the spring constant k is reduced by half, thus the numerator $B\ell k/L$ of (4) is reduced from the nominal value of 1000 to 500, and then the output response with fuzzy controller is as in Fig. 18, one can see the result of the new

method is still very good.

IV. TEST RESULTS AND DISCUSSIONS

The operation steps are summarized as follows. The first step of test is initial leveling of the balance lever arm, which is achieved by adjusting the current through the coil of force actuator. Since the lever arm weight at the stylus probe (contact with the sample) side is heavier than the other side (contact with actuator) intentionally, thus the force actuator should push down to make the balance lever arm even. The contact point of the lever arm on the load cell is installed right at the calibrated-leveling height. This adjustment process stops when the value of load cell output increases from 0 mg to 40 mg. This value for the weight discrimination can be lowered if the circuit routing condition is better, thus the noise amplitude at the load cell output can be reduced.

The next step is to load the sample on the holder which is fixed on the piezo-stage as well as XYZ-stages, and then setting the XY-stages (the resolution is 34 nm in either axis) to make the first sampled point just right under the tip of the stylus probe, then raising the piezo-stage upward until the sampled point touching with the probe. The value of the probe contact force on the sample can be obtained by the load cell. In order to make sure that the probe contacts with the sample while not destroy it, the maximum contact force is limited to 100 mg, i.e., if the magnitude of contact force is smaller than 100 mg, then moving the piezo-stage upward by one step (the resolution is 10 nm), otherwise, stop. Then by scanning the XY-stages in either x- or y-axis, and finally, the surface profile of the sample can be obtained as shown in Figs.19 (a) and (b) for side view and top view, respectively.

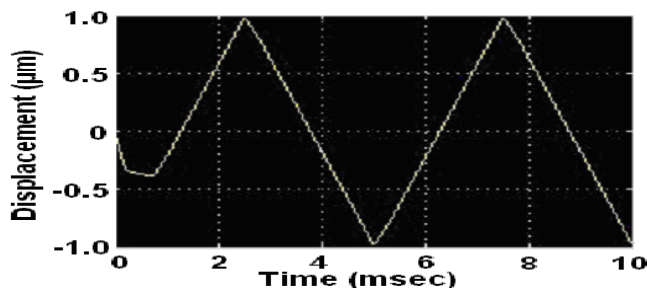


Fig. 17 The output response with fuzzy controller ($D = 0.5$ and $R/L = 3900$).

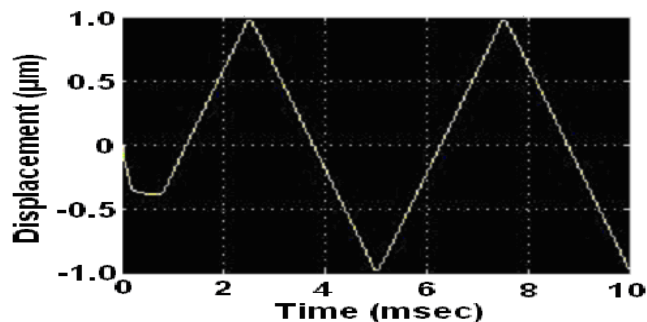
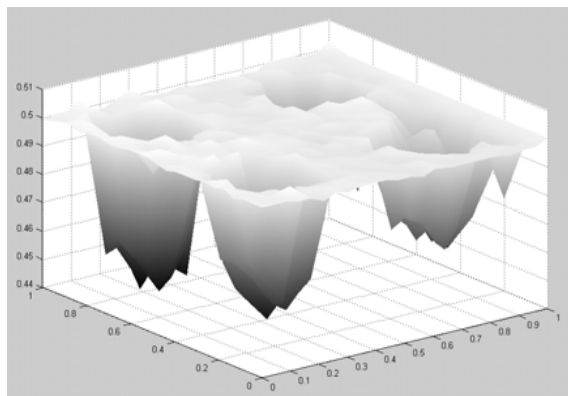
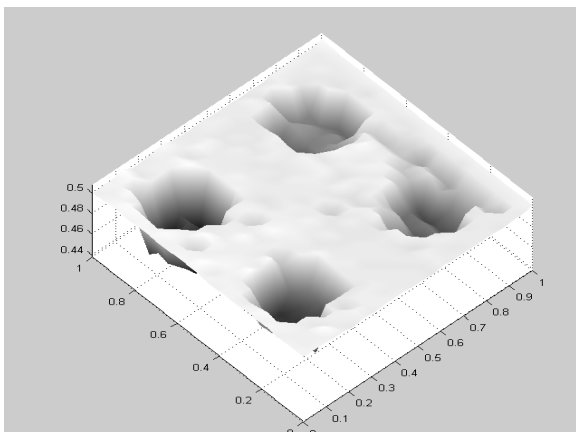


Fig. 18 The output response with fuzzy controller ($D = 0.5$ and $B\ell k/L = 500$).



(a) Side view.



(b) Top view.

Fig.19 The surface profile of a sample with the proposed method

V. CONCLUSION

This research applied fuzzy control method for a Scanning Probe Microscope (SPM) system design. In addition, the actuator hysteresis as well as parameter variation effects were taken into consideration. Comparisons with a previous work are also made, it can be seen that the system performance obtained by the fuzzy controller is much better. This improvement has been verified by MATLAB simulation and practical implementation of a surface profiler. Thus the proposed system is more robust. Finally, the profile of the object surface is displayed on a 3D graph.

ACKNOWLEDGMENT

This research was supported by National Science Council under the grants of NSC 95-2221-E-216-012, NSC 96-2221-E-216-029- and NSC 97-2221-E-216- 013-MY2.

REFERENCES

- [1] D. G. Chetwyud, X. Liu and S. T. Smith, "A controlled-force stylus displacement probe," *Precision Engineering*, vol. 19, October/November 1996, pp. 105–111.
- [2] X. Liu, D. G. Chetwyud, S. T. Smith, and W. Wang, "Improvement of the fidelity of surface measurement by active damping control," *Measurement Science Technology*, 1993, pp. 1330–1340.
- [3] M. Bennett, and J. H. Dancy, "Stylus profiling instrument for measuring statistical properties of smooth optical surfaces," *Applied Optics*, Vol. 20, No.10, 1981, pp. 1785–1802.

- [4] D. G. Chetwyud, X. Liu and S. T. Smith, "Signal fidelity and tracking force in stylus profilometry," *J. of Machinery Tools and Manufacture*, vol. 32, no.1/2, 1992, pp. 239–245.
- [5] G. Neubauer, "Force microscopy with a bidirectional capacitor sensor," *Rev. Science Instrument*, vol. 61, 1990, pp. 2296–2308.
- [6] M. Bennett, and J. H. Dancy, "Stylus profiling instrument for measuring statistical properties of smooth optical surfaces," *Applied Optics*, vol. 20, 1981, pp. 1785–1802.
- [7] J. I. Seeger, and S. B. Crary, "Stabilization of statistically actuated mechanical devices," *electro-transducers '97*, Chicago, IL, 1981, p. 1133.
- [8] G. Haugstad, and R. R. Jones, "Mechanisms of dynamic force microscopy on polyvinyl alcohol: region-specific non-contact and intermittent contact regimes," *Ultra microscopy*, vol.76, 1999, pp.77–86.
- [9] V. V. Prokhorov, and S. A. Saunin, "Probe-surface interaction mapping in amplitude modulation atomic force microscopy by integrating amplitude-distance and amplitude-frequency curves," *Appl. Phys. Lett.*, vol. 91, 2007, pp. 1063–1065.
- [10] J. M. Lin and C. C. Lin, "Profiler design with multi-sensor data fusion methods," *SICE Annual Conference 2007 in Takamatsu*, September 17-20, 2007, pp. 710–715.
- [11] P. K. Chang and J. M. Lin, "Scanning probe microscope system design with linear velocity transducer for feedback compensation," *SICE Annual Conference 2008 in Tokyo*, August 20-22, 2008, pp. 2382–2387.
- [12] H. Zhang and D. Liu, "Fuzzy modeling & fuzzy control", New York: Springer-Verlag, 2006.
- [13] P. K. Chang and J. M. Lin, "Integrating traditional and fuzzy controllers for mobile satellite antenna tracking system design," *Proceedings of WSEAS Conference on Advances in Applied Mathematics, Systems, Communications and Computers*, selected papers from *Circuits, Systems and Signals 2008, Marathon Beach, Attica, Greece*, June 1-3, 2008, pp. 102–108.
- [14] G. Bartolini, A. Ferrara, E. Usai, "Chattering avoidance by second-order sliding mode control," *IEEE Transactions on Automatic Control*, vol. 43, February 1998, pp. 241–246.
- [15] W. Perruquetti and J. P. Barbot, "Sliding mode control in engineering," CRC Press, 2002.